ENHANCEMENT OF MULTIFREQUENCY MICROWAVE PROCESSING OF CERAMICS USING MICROSTRUCTURE MODIFICATION

FINAL REPORT

J.P. CALAME
Y. CARMEL

U.S. ARMY RESEARCH OFFICE

CONTRACT/GRANT NUMBER DAAH049610344

INSTITUTE FOR PLASMA RESEARCH
UNIVERSITY OF MARYLAND
COLLEGE PARK, MD 20742

SF 298 MASTER COPY , KEEP THIS COPY FOR REPRODUCTION PURPOSES

REPORT DOCUMENTATION PAGE

Form Approved
OMB NO. 0704-0188

1. AGENCY USE ONLY *(Leave blank)*	2. REPORT DATE	3. REPORT TYPE AND DATES COVERED
		Final 8/1/96 - 1/31/97

4. TITLE AND SUBTITLE
Enhancement of Multifrequency Microwave Processing of Ceramics Using Microstructure Modification

5. FUNDING NUMBERS
DAAH04-96-1-0344

6. AUTHOR(S)
J. P. Calame
Y. Carmel

7. PERFORMING ORGANIZATION NAMES(S) AND ADDRESS(ES)
Institute for Plasma Research
University of Maryland
College Park, MD 20742-3511

8. PERFORMING ORGANIZATION REPORT NUMBER
N/A

9. SPONSORING / MONITORING AGENCY NAME(S) AND ADDRESS(ES)
U.S. Army Research Office
P.O. Box 12211
Research Triangle Park, NC 27709-2211

10. SPONSORING / MONITORING AGENCY REPORT NUMBER
ARO 35647.1-MS-II

11. SUPPLEMENTARY NOTES
The views, opinions and/or findings contained in this report are those of the author(s) and should not be construed as an official Department of the Army position, policy or decision, unless so designated by other documentation.

12a. DISTRIBUTION / AVAILABILITY STATEMENT
Approved for public release; distribution unlimited.

12 b. DISTRIBUTION CODE

13. ABSTRACT *(Maximum 200 words)*

A method to increase the loss tangent in a ceramic green body by modifying the nature of the interparticle contact areas is described. Such an increase in loss tangent, achieved through modifying the ceramic microstructure with material of the same chemical composition as the parent ceramic, will make rapid microwave sintering possible without altering the chemical stability of the system. For research purposes, the method of infusing a ZnO green body with a 0.053 M zinc acetate solution was selected. Following the infusion, a gel of hydrous $Zn(OH)_2$ is formed in the pores through the action of aqueous ammonia, and ZnO is created by subsequent heating. A test sample was fabricated and subjected to this treatment. Dielectric properties in the 0.2-10.0 GHz regime were measured before and after treatment. The test sample showed a substantial increase in dielectric loss that is consistent with improved interparticle contact.

14. SUBJECT TERMS	15. NUMBER IF PAGES
Microwave sintering, ceramics, dielectric loss, ZnO	17
	16. PRICE CODE

17. SECURITY CLASSIFICATION OR REPORT	18. SECURITY CLASSIFICATION OF THIS PAGE	19. SECURITY CLASSIFICATION OF ABSTRACT	20. LIMITATION OF ABSTRACT
UNCLASSIFIED	UNCLASSIFIED	UNCLASSIFIED	UL

(1) List of Manuscripts:

"Electric Field Intensification in Spherical Neck Ceramic Microstructures During Microwave Sintering," J.P. Calame, K. Rybakov, Y. Carmel, and D. Gershon, *Ceramic Transactions* **80**, (American Ceramic Society, Westerville, OH), in press (1997). See Appendix A for preprint.

(2) Scientific Personnel Supported:

Dr. Yuval Carmel, Senior Research Scientist
Dr. Jeffrey P. Calame, Assistant Research Scientist

(3) Report of Inventions: N/A

(4) Scientific Progress and accomplishments: See main body of report beginning on page 3.

(5) Technology Transfer:

Some of the research on the role of microstructure on losses in dielectrics is finding use in a Phase I SBIR from NSF at Physical Sciences Inc., Alexandria, VA. The title of their work is "Improved Microwave Absorbing Insulator-Conductor Composites with Tailored Frequency Response." We are also working with the Center for Remote Sensing, Fairfax, VA, on a Phase II DOD SBIR on commercializing the two-frequency microwave sintering technique.

I. Overview

High heating rate microwave sintering of ceramics can be used to limit grain growth, preserve tailored microstructures that create specific mechanical and electrical properties, prevent undesirable phase and chemical transformations in complex systems, and accelerate fabrication times. For this technology to become practical for a wide range of advanced ceramics, several issues must be addressed. First, the initial microwave loss prior to sintering must be made sufficiently high to allow energy absorption, without negatively affecting final mechanical properties or chemical stability. This is an issue for many important ceramics such as Al_2O_3 and Si_3N_4, which are normally low loss. Second, high heating rates require the use of two simultaneously applied microwave sources with widely separated frequencies to control thermal gradients (by deposit energy selectively into internal and surface regions via the skin depth phenomenon). For this spatial segregation to occur, the material must be sufficiently lossy (for a given physical size of the ceramic body being processed) or both sources will penetrate fully into the material. Once again a means to tailor the dielectric loss without greatly affecting the overall ceramic properties is required.

However, the critical issue for sintering is not only the lossyness of the fully dense body, but rather the lossyness of the porous ceramic at various stages of densification. The dielectric constant and loss of ceramics both decrease with increasing porosity. Typical green bodies have about 50% porosities. For some materials, the effect of porosity is to reduce the lossyness in an approximately linear fashion, which could retain a useful level of loss at the 50% porosity starting point. As the ceramic densifies, the situation obviously improves further. On the other hand, certain other materials of great practical importance, such as aluminum oxide and zinc oxide, exhibit a much more dramatic, nonlinear decrease in loss as the porosity increases (e.g. a 90% reduction in loss with 50% porosity). This not only makes it difficult to couple microwave energy into the material, but it also largely negates the benefits of the two-frequency thermal gradient control technique throughout a significant portion of the densification process. The cause of this abnormally rapid decrease in microwave loss with increasing porosity in these types of materials is poor electrical contact between the ceramic grains [1], due to irregular surfaces and intergranular cracks.

In this Short Term Innovative Research (STIR) program we performed an initial experiment and completed theoretical investigations to address the problem of low microwave loss in porous materials and the relation between microstructure and electromagnetic properties. We were able to substantially increase the dielectric loss in a 66% dense body of ZnO by infusing the existing micron-scale microstructure with a nanoparticle gel using chemical precipitation techniques. The small particles can act as lossy dielectric bridges between the irregular surfaces of the larger particles, improving electrical contact and thus the overall loss. The results of a theoretical computation of this type of effect are shown in Fig. 1. This effect is intimately related to the physics of microwave loss in spatially inhomogeneous bodies and has a far greater impact on the loss than what would be expected from the trivial increase in starting density alone (by means of the larger fill factor afforded by the additional small particles). By achieving the increased and controllable lossyness using additives of the same intrinsic composition as the parent ceramic (with a different morphology, however), possible undesirable changes in chemical compositions or degradations in chemical stability associated with some conventional sintering agents can be avoided. Such additions of small grains could also act to arrest large intergranular cracks in

finished ceramic parts, which improves the mechanical properties. The significance of our proposed activity is due to its potential to open innovative approaches to the rapid processing of high performance ceramic materials of relevance to ARO. Examples include transparent armor, high temperature rocket and engine components where light weight and high strength are also critical, components subject to wear such as bearings, and composites.

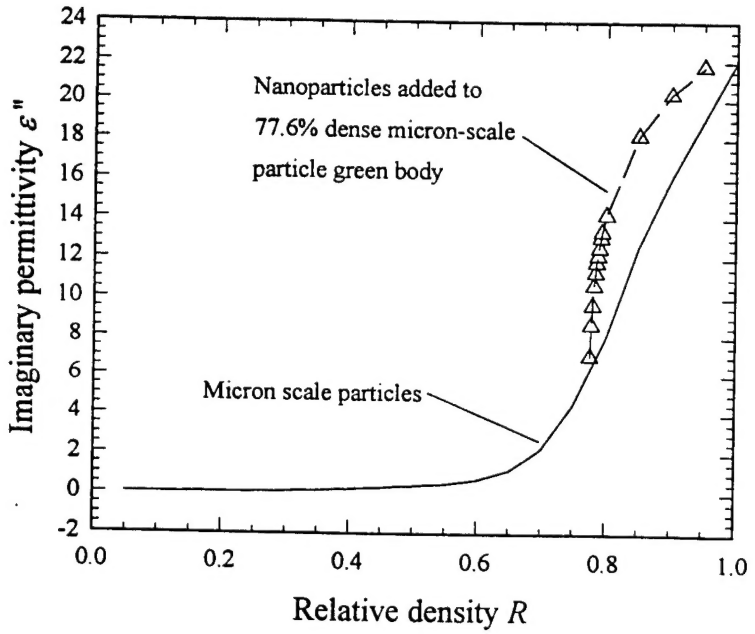

Figure 1. Computed effect at 2.45 GHz of microstructure modification with nanoparticles, hypothetically performed on a 78% dense green body composed of micron-scale ZnO particles (triangles). The solid line shows the behavior of a green body composed of micron-scale particles only.

II. Description of Research Results

The lack of significant electrical percolation, due to the physically rough surfaces of the individual particles, has been shown to inhibit the overall loss of a porous material, in spite of high relative density and high intrinsic losses in the particles themselves [1]. Nanoparticles placed selectively in the interparticle contact zones will increase the contact surface area and the quality of the electrical contact by strictly physical (as opposed to chemical) means. In future research we plan on developing techniques to coat individual 1 μm ceramic grains with a thin layer of nanoparticles, so that this modified material can be used as a new raw material in commercial applications. However, for the purposes of this initial STIR program, we decided to create nanoparticle or gel condensations directly inside a porous, lightly-sintered ceramic body created with ordinary ceramic grains. In this manner the basic concept of microstructure modification was tested directly.

Three test samples of ZnO were prepared by cold isostatically pressing 1-2 μm grain size powder to 37 MPa without the use of binders. The samples were conventionally pre-sintered at 15 °C/minute until a temperature of 860 °C was reached; at this time the samples were allowed to naturally exponentially cool over a period of about 45 minutes. The resulting samples have a relative density of about 66 % (porosity 34 %), and were mechanically stable enough to withstand soakings in aqueous solutions. The samples were lapped on both sides, weighed, and initial dielectric measurements from 0.2-10 GHz were taken at room temperature using a commercial coax-to-surface probe and a vector network analyzer (both made by HP). A single sample with median properties was selected to receive the microstructure modification. It had a mass of 28.594 g and a volume of 7.68 cm^3.

A process based on zinc acetate, $Zn(C_2H_3O_2)_2$, was chosen to create a ZnO gel in the open porosity network of the green body. The idea is to infuse the pores with a zinc acetate solution, and subsequently convert the dissolved zinc acetate to a gel precipitate of hydrous zinc hydroxide by additions of aqueous ammonia. Depending on the conditions of the reaction, such as pH, concentration of acetate, and temperature, the gel could consist of large agglomerates of individual particles, each anywhere from 5 nm to 100 nm in diameter, or if the concentration of Zn^{2+} is very weak, isolated nanoparticles could be created. The reaction is

$$Zn(C_2H_2O_2)_2(aq) + 2NH_4OH \rightarrow Zn(OH)_2(s) + 2[NH_4]^+ + 2[C_2H_3O_2]^-$$

Care has to be taken to avoid raising the pH too high, or the $Zn(OH)_2$ will re-dissolve to form a zincate ion, $[Zn(OH)_4]^{2-}$. In addition, if too much ammonia is present, then a soluble $[Zn(NH_3)_4]^{2+}$ will form as well. Careful control of the pH and the relation between the concentrations of $[NH4]^+$ and Zn^{2+} is therefore necessary.

Based on the porosity and density of ZnO, we decided to use an acetate solution which is 0.053 M in Zn^{2+}, which if fully precipitated in the pores of the test sample would produce a 0.5% increase in relative density of the green body. Such an increase would by itself do little to increase the lossyness by conventional mixing laws, but if the gel improves percolation in the fractal-boundary, interparticle contact zones, then a substaintial increase in loss could be expected theoretically [1]. A 0.053 M Zn^{2+} solution was prepared using 22.4 g zinc acetate dihydrate per 100 mL of solution. The pH of this solution was 5.50. The test sample was placed in 100 mL of this solution and allowed to soak for 48 hours at room temperature. After 24 hours, some spontaneous formation of $Zn(OH)_2$ was observed in the liquid near the sample surface, which was probably caused by the slightly basic nature of ZnO itself. Although this gelling does not harm the process, and in fact may have specific advantages, in future experiments it would be desirable to avoid this spontaneous gellation to better understand competing processes.

In order to closely evaluate the effect of pH on gelling and re-dissolution of the zinc hydroxide, a titration analysis was performed on a sample of 50 mL of the 0.053 M zinc solution, using 1.5 M aqueous ammonia (NH_4OH) as the titrant. A plot of the results are shown in Fig. 2. An initial fine precipitate of hydrous $Zn(OH)_2$ forms with even the smallest additions of NH_4OH, and the amount of precipitate reaches a maximum at a pH near 7.0. Further additions of NH_4OH resulted in rapid re-dissolution of the precipitate, which completely disappeared at pH 11.3. A true gellation point, in which a viscous network of precipitated material forms a single spanning cluster throughout the volume of the beaker, was not observed in this system. Furthermore, the titration curve is very gentle and lacks clear transition points. While at the higher values of pH one would certainly expect dissolution due to the formation of the zincate ion $[Zn(OH)_4]^{2-}$, the

premature disappearance of precipitate is probably due to the formation of the $[Zn(NH_3)_4]^{2+}$ complex ion. In any case, a substantial amount of $Zn(OH)_2$ remained at a pH of 8.0, so this value was chosen for the initial gelling conditions.

The sample, saturated with zinc acetate solution (which was now at a pH of 5.80), was placed into 150 mL of pure water and small amounts of dilute aqueous ammonia were added to raise the liquid pH to 8.00. The sample was placed aside soaking at that pH for 24 hours. After this time the pH had dropped to 6.8, which is nearly ideal based on the titration curve. The sample was removed and dried at 80 °C in air for 12 hours, then transferred to a Soxhlet extraction apparatus. The sample was treated with water extraction for 24 hours to leach out the soluble $[NH_4]^+$ and $[C_2H_3O_2]^-$ ions and dried at 80 °C for another 24 hours. To convert the hydrous $Zn(OH)_2$ to ZnO, the sample was heated at 15 °C/min. to 750 °C in air. This destroyed any residual ammonium acetate.

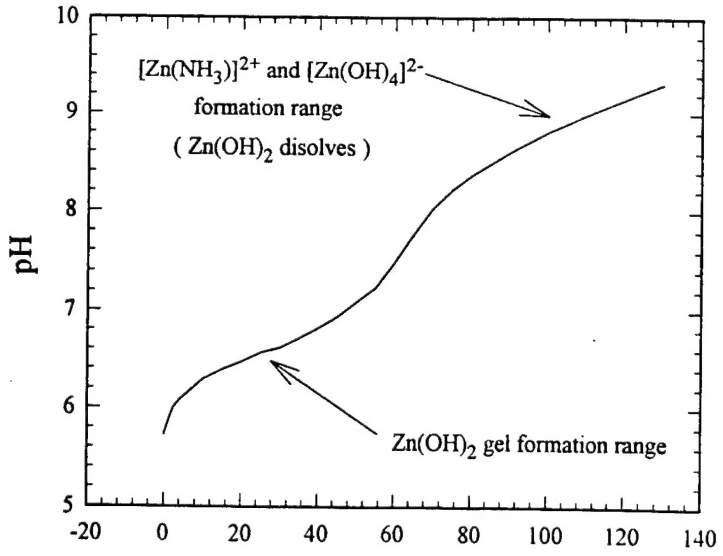

Figure 2. Titration curve for zinc acetate solution.

The sample was subjected to a second set of microwave measurements to determine the complex dielectric constant ($\varepsilon = \varepsilon' - j\varepsilon''$) over the 0.2-10.0 GHz frequency range after treatment. The results, along with the data before the sample treatment, are shown in Fig. 3. The imaginary part of the dielectric constant ε'' represents the electrical loss, which is the basis for power absorption in microwave processing. The data shows increased loss over the entire frequency band, with the greatest effect occurring below 1.0 GHz. At 2.45 GHz, a common processing frequency, ε'' increases from about 0.4 to 0.6. At lower frequencies the loss approximately doubles. Although the change in loss decreases as the frequency is raised, the results are not consistent with a simple impurity-based increase in dc conductivity, which would give a *1/f* dependence to the excess loss. The real part of the dielectric constant also increases with the

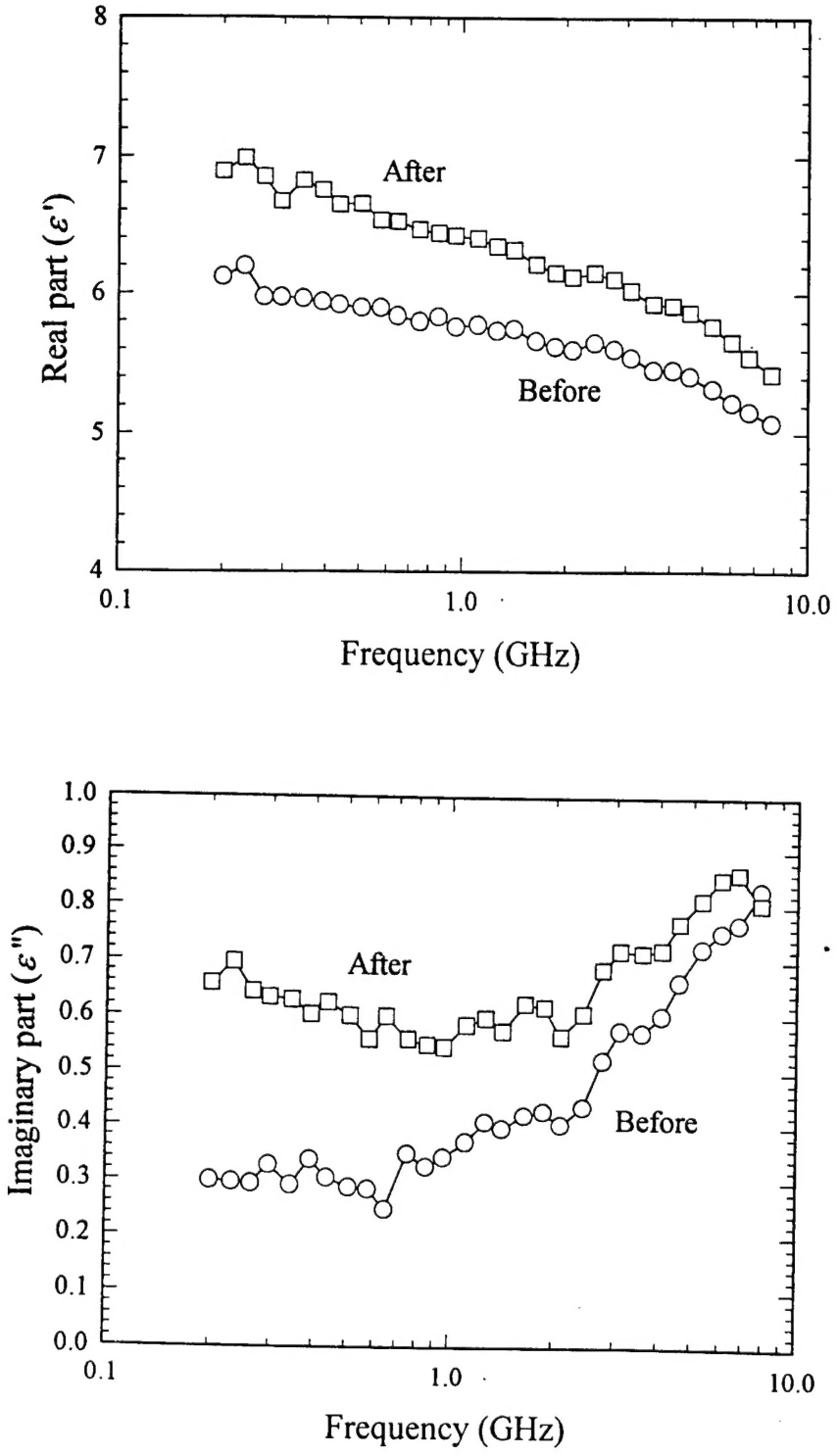

Figure 3. Experimental measurements of the dielectric properties of the ZnO sample before and after microstructure modification.

treatment, and the frequency dependence of the change in dielectric constant due to treatment is less dramatic. The increase in ε' is more consistent with a change in microstructure resulting in greater interparticle contact than with impurity effects. Microstructure analysis with electron microscopy will be needed in future research to provide further confirmation. In order to investigate the role of changes in microstructure on electromagnetic properties in porous ceramics, a detailed theoretical study was performed. Finite difference electromagnetic solution techniques were applied to representative models of spherical neck ceramic microstructures. It was determined that large enhancements in electric fields (factors of 10-100) are possible during microwave sintering in the interparticle contact areas of the microstructure [2]. As a result, the overall dielectric properties are very sensitive to changes in the structure and chemistry of the particle contact regions, in spite of the small overall volume of these areas. A copy of our paper exploring this topic is provided in Appendix A.

In retrospect two types of microstructure modification that would increase the interparticle contact are possible in the experiment. The first is the direct precipitation of extra material from the zinc acetate solution directly onto the pore surfaces, including the contact zones. This was the intended process. The second process would involve dissolution of existing ZnO from the micron scale particles by virtue of the amphoteric nature of ZnO coupled with the acidic nature of the zinc acetate solution, followed by re-precipitation into the contact zones. This type of structural change is known as solution coarsening. The driving force for of mass transport is due to differences in solubility s between surfaces with different radii of curvature r, and is related to chemical potential effects. The modified solubility is given by

$$s = s_0 \exp\left(\frac{2\gamma_{SL}V_m}{R_g Tr}\right)$$

where s_0 is the solubility of a flat plate of the solid phase, γ_{SL} is the solid-liquid interfacial energy, V_m is the molar volume of the solid, R_g is the ideal gas constant, and T is the temperature [3]. The main part of the green body particles have positive radii of curvature, so they are more soluble than a flat plate. On the other hand, crevices and necks between particles have negative radii so their solubility is especially low and material tends to accumulate there. By the same mechanism, small nanoparticles created from the reaction between NH_4OH and zinc acetate tend to dissolve (due to small radius of curvature) and re-precipitate in the areas of the interparticle neck. From the practical standpoint of increasing the loss by microstructure modification, it makes little difference which mechanism is responsible. However, for the future development of new materials it will be important to ascertain the relative contributions of these two processes to observed dielectric changes with electron microscopy.

III. References

[1] J.P. Calame, A. Birman, Y. Carmel, D. Gershon, B. Levush, A.A. Sorokin, V.E. Semenov, D. Dadon, L.P. Martin, and M. Rosen, "A Dielectric Mixing Law for Porous Ceramics Based on Fractal Boundaries," *Journal of Applied Physics*, 80, pp. 3992-4000 (1996).

[2] J.P. Calame, K. Rybakov, Y. Carmel, and D. Gershon, "Electric Field Intensification in Spherical Neck Ceramic Microstructures During Microwave Sintering," *Ceramic Transactions* **80**, (American Ceramic Society, Westerville, OH), in press (1997).

[3] C.J. Brinkner and G.W. Scherer, Sol-Gel Science: *The Physics and Chemistry of Sol-Gel Processing*. (Academic Press, San Diego, 1990), p. 360.

Appendix A

ELECTRIC FIELD INTENSIFICATION IN SPHERICAL NECK CERAMIC MICROSTRUCTURES DURING MICROWAVE SINTERING

J.P. Calame, K. Rybakov†, Y. Carmel, and D. Gershon
Institute for Plasma Research, University of Maryland, College Park, MD 20742.
† Institute of Applied Physics, Nizhny Novgorod, 603600, Russia.

INTRODUCTION

During microwave sintering, the electric field distribution within a ceramic body on a macroscopic scale is determined by a combination of the operating frequency, the applicator type, the manner in which the electromagnetic waves illuminate the sample, and the sample shape, permittivity and permeability. Within the sample, the spatial variation of the electric field occurs on length scales comparable to the wavelength or skin depth of the electromagnetic waves within the ceramic. However, this is only true if one is considering the variation of fields over volumes much larger than the characteristic feature sizes of the microstructure (i.e. grain sizes, rough surfaces of grains, and interparticle contact zones). Within the microstructure itself, the electric field exhibits violent variation in magnitude and direction. Furthermore, the electric field in certain areas of a realistic microstructure can be orders of magnitude stronger than the spatially averaged electric field, and it can exhibit preferred polarization directions despite being illuminated by a randomly polarized electric field. In this paper, calculations of electric field distributions within ensembles of ceramic particles, joined by spherical necks to mimic the middle stages of sintering, will be presented. The relation between the predicted electric field enhancements and current theories of microwave sintering will be discussed.

ELEMENTARY THEORY

In a volume of material undergoing microwave sintering, the electric field present within a volume V can be expressed in terms of temperature rise dT/dt. The governing relation is

$$c\,\rho_m V \frac{dT}{dt} = \frac{1}{2}\omega\varepsilon_0 \int_V \varepsilon'' |E_l|^2 dV \xrightarrow[V \text{ is large}]{} = \frac{1}{2} V \omega \varepsilon_0 \varepsilon_m'' |E|^2 \qquad (1)$$

where ρ_m is the mass density, c is the specific heat, ω is the frequency, ε_0 is the permittivity of free space, ε'' is the imaginary part of the relative permittivity of the differential integration volume dV, and E_l is the electric field inside dV. If the volume of interest is considerably larger than the size scale of the individual microstructure elements, then one can recast the RHS in terms of ε_m'', an effective imaginary permittivity of the heterogeneous mixture consisting of ceramic and air, and a spatially averaged electric field amplitude E. To determine the local electric field E_l within a microstructure characterized by average field E, in general it is necessary to perform a finite difference simulation of a realistic microstructure. In some cases an analytic solution is possible. For example, in a system consisting of layers of air and ceramic in planes perpendicular to the applied field, the field inside the ceramic is $1/\varepsilon$ lower than the field in the air due to continuity of normal electric displacement [1,2].

FIELD INTENSIFICATION

However, in some very common microstructures the fields inside certain ceramic regions can greatly exceed not only the fields in the pores, but also the applied field. This occurs by geometrical focusing effects. A highly relevant microstructure of this type is a pair of ceramic spheres joined by a spherical neck, as shown in Figure 1. The neck radius of curvature ρ is given by $x^2/(2R)$, where x and R are neck and sphere radii. As long as the physical size of the microstructure under investigation is much smaller than either a wavelength or skin depth in the ceramic at the frequency of interest, electrostatic finite difference field solution methods can be used to obtain detailed information regarding the electric field structure.

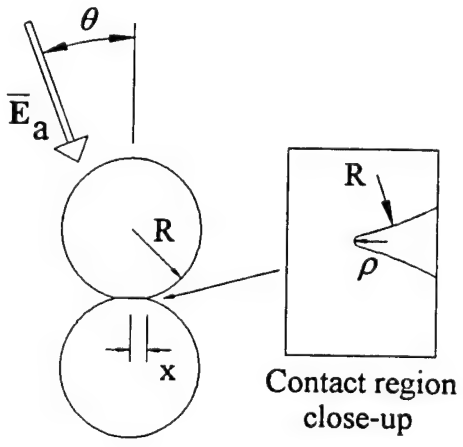

Figure 1. Diagram of the spherical neck geometry

In the finite difference procedure, a model space is created from simulation cells that are filled with either air or ceramic to form the desired microstructure, and appropriate permittivities are assigned to cells (in general the cells need not be uniform in size). The non-zero frequency regime is handled through the use of complex permittivities and potentials. An applied electric field is created by assigning a potential of zero on the bottom of the model space, and a potential of one at the top (opposite face). Mirror boundary conditions are applied to the other four sides. Internal potentials are subsequently found at the vertices that define each cell by either iteration or sparse matrix inversion, and electric fields are computed afterwards from potential gradients.

Finite difference simulations of the structure in Figure 1 have been carried out in three dimensions for a variety of angles θ, where θ is the angle between the principle axis joining the spheres and the direction of the applied field E_a. In these simulations uniform cubical mesh cells were used, and the model space was composed of 32x64x64 (x,y,z) cells. The geometry was constructed such that the center of the contact region was located at the model space center (x=16, y=32, z=32), the applied field was directed along the z axis, and the axis of joining was located in the y-z plane (making an angle of θ with respect to the z-axis). Spheres of radius R = 14 were used, and the inter-sphere separation was chosen to give a neck radius x equal to $0.26R$. To study two representative materials, dielectric permittivities representative of either hot Al_2O_3 at 35 GHz (ε = 10 -1.0j) or hot ZnO at 2.45 GHz (ε = 40-20j) were used for the ceramic cells.

For θ = 0°, intensified fields inside the ceramic are found throughout the circular inter-particle contact zone, with the highest fields located directly adjacent to the outer circumference of the neck. The peak internal fields are significantly greater than the applied field. Lesser peak intensities, with a similar spatial pattern within the neck, are found for other values of θ. A plot of this effect for the neck region in two materials is shown in the top graph of Figure 2. For the case with θ = 90°, the peak field in the neck region is less than the applied field and less than the spatially averaged field throughout the volume of ceramic. The external field (in air) also follows a similar pattern but with higher intensity, as can be seen in the middle graph of Figure 2. Finally, the peak internal magnitude of the electric field squared (E^2) in the neck region, divided by the value of the field squared field spatially averaged over the entire volume of ceramic material (not air), is shown as a function of angle in the bottom graph of Figure 2. This is an important graph, since the spatially averaged E^2 in the ceramic grains by themselves is directly related to the average power density and thus the heating rate, and it can be calculated from experiments. Knowing this, the peak field in the ceramic due to intensification can be determined from the plots, as well as the peak external field.

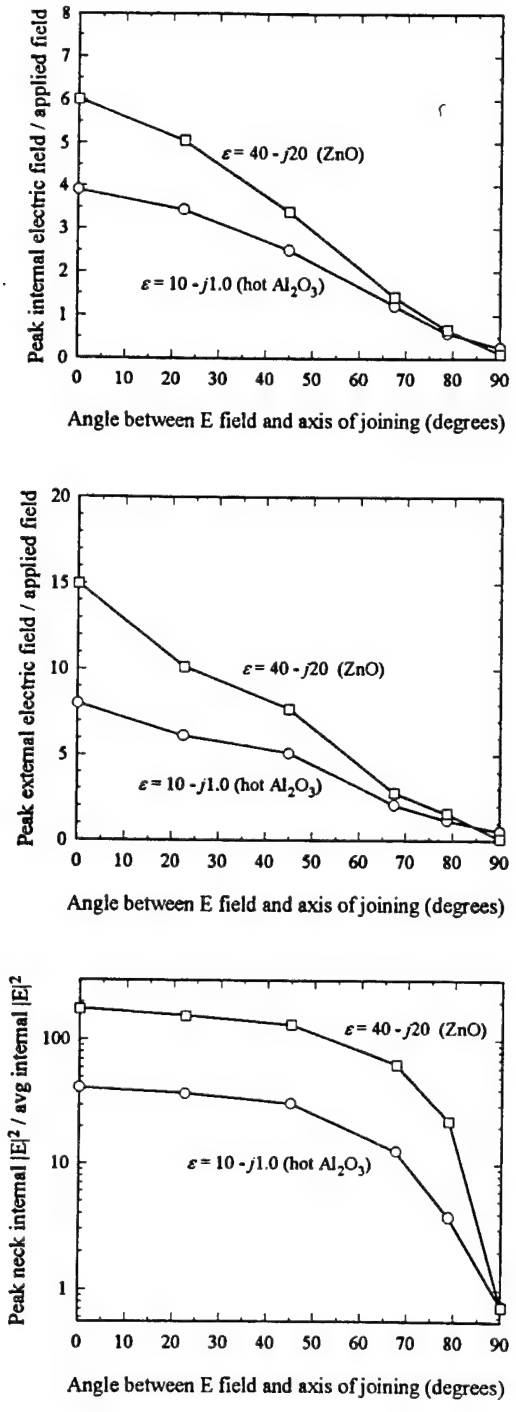

Figure 2. Results of the 3D simulations for $x/R = 0.26$ and various values of θ.

For the case with $\theta = 0°$, a variable mesh, 2D axis-symmetric simulation of high accuracy was performed, and the results are shown in Figure 3. The simulations typically used 230 radial cells by 170 axial cells, with a great concentration of cells in the neck region to accurately model the radius of curvature ρ in Figure 1. The agreement between these more accurate simulations and the 3D versions is quite good at $x/R = 0.26$. For Al_2O_3, peak internal fields for relevant values of x/R are 3-8 times larger than the applied field, and in ZnO the intensification factor is 10-30 times. The ratio of the deposited power density (proportional to $\varepsilon'' E^2$) at the peak field location divided by the average power density in the entire ceramic portion of the model is also plotted in Figure 3. For Al_2O_3 local power densities can be 100 times greater than the average value, and in ZnO the factor is over 4000. These factors far exceed previous estimates [1,2]. Corresponding peak external fields were found to be in the range of 10-15 for Al_2O_3 and 30-60 for ZnO.

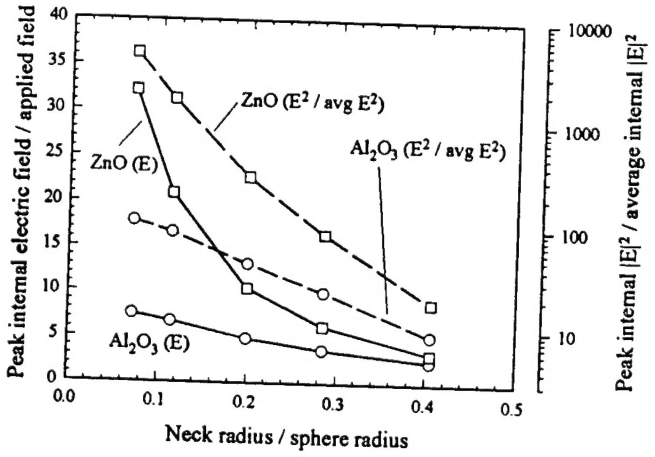

Figure 3. Results of 2D axis-symmetric, variable-mesh calculations for $\theta = 0°$.

To investigate intensification in a densifying microstructure, a simulation of spheres in a simple cubic array (with contact and neck formation allowed) was performed for the case of ZnO. A 3D model space with 80 cells per side was used. In this type of simulation the ceramic mass in the model space remains constant, and thus the model space actually is forced to shrink just as in a real material. Like in the previous studies, peak fields in the ceramic and pores can be computed, and the results are shown in Figures 4 and 5. In addition, the electrostatic energy, given by the volume integral of $0.5\varepsilon_0\varepsilon' |E|^2$, can be explicitly calculated as a function of relative density. The results of this type of procedure, converted to an energy per gram of material (ZnO density = 5.61 g/cm^3), are also plotted.

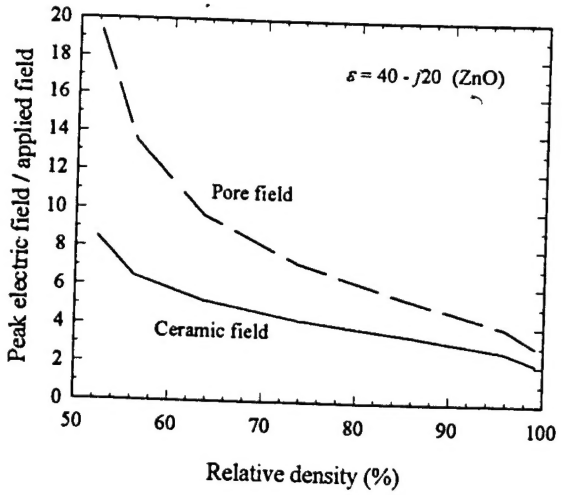

Figure 4. Results from the spheres in a simple cubic array geometry.

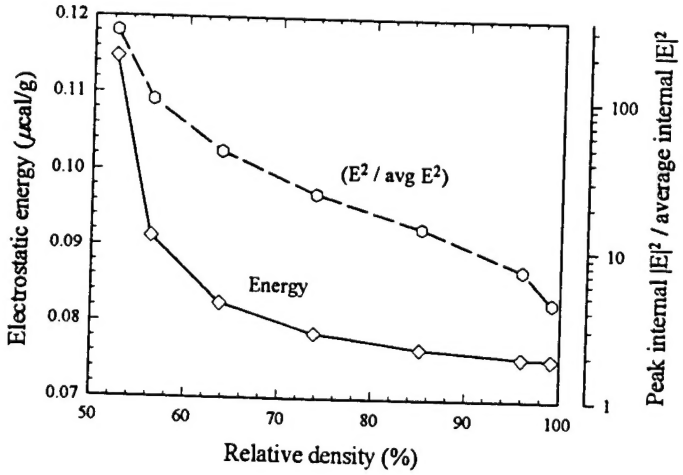

Figure 5. Additional results from the spheres in a simple cubic array geometry. For the energy calculation, a constant 1 kV/cm spatially averaged field was assumed in the ceramic grains.

CONCLUSIONS

Several conclusions relevant to microwave sintering can be drawn from this work. First, in spite of the intensification, significant differential thermal gradients still cannot be maintained across micron scale particles, as shown by Johnson [3].

The time constants of micron-scale particles are simply too small, resulting in gradients of no more than 1 μK for even a 100 K/min heating rate. Second, although densification causes a decrease in electrostatic energy of a porous ceramic [1], calculations in the simple cubic lattice realistic microstructure reveal this effect is negligible (about $4x10^{-8}$ cal/g for ZnO with a 1kV/cm average field in the ceramic grains) compared to conventional surface tension-based sintering driving forces (about 1 cal/g for 1 micron particles). Even in a microstructure composed of alternating ceramic and air layers with a perpendicularly applied field, where there is a great deal of pore electrostatic energy, the energy change under the same conditions is $3x10^{-6}$ cal/g, corresponding to only 0.01 psi effective sintering pressure. Third, with average fields of 1kV/cm, peak pore fields can be as high as 10-60 kV/cm, which are large enough to cause microscopic breakdown and plasma formation at atmospheric pressure [1]. This could lead to altered sintering characteristics normally associated with deliberate plasma-microwave sintering.

Finally, and perhaps most importantly, in the pondermotive material flow theory [4] the flow effect is proportional to E^2, and thus flow rates can be 30-4000 times larger than previously estimated as a result of intensification. Unlike in the simple force calculations based on electrostatic energy (as done above), the fields are hypothesized to apply forces only on charged vacancies concentrated near the particle surfaces, rather than being distributed over all of the atoms in the solid. This effectively amplifies the radiation pressure to create non-negligible surface flows. Furthermore, the flow pattern on a sphere is quadrupolar in shape, leading to a "rectification" of flow in response to an alternating electromagnetic field of fixed polarization axis. One of the arguments against this theory is that with a *randomly* polarized electromagnetic field like that in a multimode cavity, favorable flows will be negated (undone) at a later time as the axis of polarization changes. The 3D calculations described in this work illustrate two effects that weaken this argument. First, the value of $|E|^2$ in a spherical neck is a strong function of the field application angle θ. When $\theta = 0°$, a strong intensification will occur resulting in flows. For a polarization of $\theta = 90°$, which would create negating flows, the value of $|E|^2$ is about two orders of magnitude smaller. More importantly, the polarization direction of the intensified field within the ceramic neck remains nearly aligned with the axis of joining (axis connecting the centers of the spheres), even for electric field application angles as large as $\theta = 80°$. Thus any favorable flows occurring when $\theta = 0°$ will persist even when θ becomes large, since the internal polarization of the field is nearly constant with respect to the axis of joining. Specific simulation results associated with this effect for the ZnO dielectric are shown in Table 1. The relative magnitude of the favorable flow is proportional $E^2\cos^2\theta_d$, where E is the peak internal field strength in the neck region (top graph

in Figure 2). This flow quantity is normalized in the table to 1.0 for $\theta = 0$. Similarly, the relative unfavorable flow is proportional to $E^2\sin^2\theta_d$.

Table 1. Calculations of Internal Field Directions for ZnO Spherical Neck

Illumination Angle θ (degrees)	Deviation Angle of Internal E to Axis of Joining θ_d (degrees)	$\cos^2\theta_d$ (%)	Relative Favorable Flow	Relative Unfavorable Flow
0	0.0	100	1.0	0.0
22.5	12.6	95.2	0.66	0.033
45	13.2	94.8	0.41	0.022
67.5	8.5	97.8	0.061	0.0013
78.75	1.8	99.9	0.016	1.6×10^{-5}
90	80.0	3.0	8.3×10^{-6}	2.7×10^{-4}

By the time the deviation angle becomes large, the field intensification decreased greatly, so the large deviation angle and undesired ratio of favorable to unfavorable flow does not matter. The effect is essentially due to the spherical neck acting like an electric field channel or pipe, which forces the field through the neck along the axis of joining. More precise calculations on the magnitude and direction of pondermotive flows which exist in a spherical neck geometry are under way at the present time.

ACKNOWLEDGMENTS

This work was primarily supported by the Air Force Office of Scientific Research under a MURI grant. Support from an Army Research Office STIR is acknowledged, and a NATO Linkage Grant supported the visit of K. Rybakov.

REFERENCES

1. T. Saji, in "Microwave Processing of Materials V," M.F. Iskander, J.O. Kiggans, Jr., J.C. Bolomey, editors (Materials Research Society, Pittsburgh, 1196), Mat. Res. Soc. Proc. Vol. 430, p. 15.

2. T. Meek, J. Mat. Sci. Lett. 6, 638 (1987).

3. D.L. Johnson, J. Am. Ceram. Soc. 74, 849 (1991).

4. K. Rybakov and V.E. Semenov, Phys. Rev. B52, 3030 (1995).